Phase Equilibrium Behavior of the Ethane + Dimethyl Sulfoxide and Ethane + Quinoline Binary Systems

Amita Trehan, James P. Kohn,* and David G. Bibbs

Department of Chemical Engineering, University of Notre Dame, Notre Dame, Indiana 46556

The equilibrium vapor pressure, liquid-phase composition, and liquid-phase molar volume are presented for ethane + dimethyl sulfoxide and ethane + quinoline at 298.15, 308.15, and 318.15 K. Also, the pressure, liquid-phase compositions, and liquid-phase molar volumes on the liquid$_1$ + liquid$_2$ + vapor locus are presented. The termination of these loci are located and characterized.

Introduction

The effective design of most separation processes demands reliable phase and volumetric data. Phase equilibria of various hydrocarbons with ethane as a solvent gas near its critical point have been investigated by many researchers. Many of these ethane + hydrocarbon binary systems have been found to exhibit complex phase behavior in regions near the critical point of the lighter component. The phenomenon of partial miscibility was first observed by Kuenen and Robson (*5*) in the ethane + methanol binary and has been investigated extensively by many researchers since then. The study of the phase equilibrium behavior of ethane and hydrocarbons has been conducted by Kohn and co-workers (*4*, *10*-*12*), ethane + straight chain hydrocarbons by Specovius et al. (*13*), ethane + pyrimidine and ethane + quinoxaline by Yamamoto et al. (*16*, *17*), ethane + aromatics by Berlin and co-workers (*1*) and Jangkamolkulchai et al. (*3*), ethane + *n*-alkylbenzene series by Li (*7*), ethane + decahydronaphthalene by Nitschke (*8*), and ethane + aromatics and ethane + *n*-alkanols by Brunner (*2*) and Lam et al. (*6*). The above studies have revealed that many binary systems of ethane exhibit regions of immiscible behavior which are characterized by upper (type K point indicates here a liquid and vapor phase are identical in the presence of a noncritical liquid phase) and lower (LCST or Q point indicates coexistence of four phases) bounds. In the ethane + paraffin binary mixtures there is only a few percent difference in the composition of the phases. Hence, only small regions of immiscibility exist. In less soluble systems, such as ethane + substituted aromatics, the regions of immiscibility can be larger and the LCST point may not occur. Instead the L-L-V region extends down to the quadruple point (Q, S-L-L-V), which is analogous to the triple point of the pure component.

In order to further our understanding of the partial miscibility phenomenon and help elucidate the nature of phase equilibria, binary systems of dimethyl sulfoxide (DMSO) and quinoline with ethane were investigated in the present work. L-V equilibria have been measured along the 298.15, 308.15, and 318.15 K isotherms, in the pressure range of 0-70 bar for quinoline and 0-105 bar for DMSO. L-L-V-E data have been obtained over the entire range of immiscibility, i.e., between the K point and the Q point.

Experimental Section

A detailed description of the apparatus and the procedure is given by Puri and Kohn (*9*). The essential ap-

* To whom correspondence should be addressed.

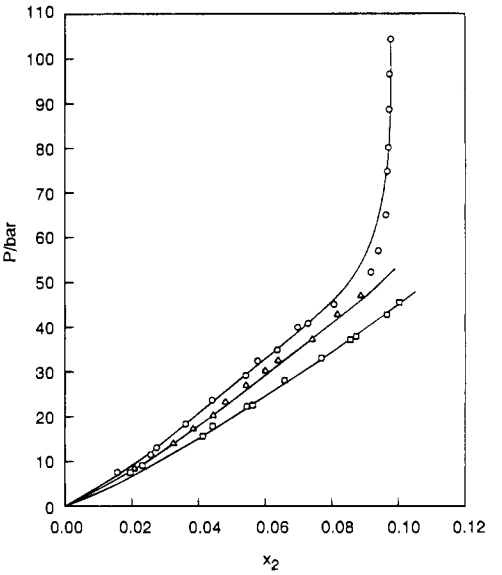

Figure 1. Isothermal pressure versus ethane mole fraction x_2 in ethane (2) + DMSO (1) in the L-V region: □, T = 298.15 K; △, T = 308.15 K; ○, T = 318.15 K.

Table 1. Smoothed Values of Liquid-Phase Composition and Liquid Molar Volume V as a Function of Pressure for the Binary System Dimethyl Sulfoxide (1) + Ethane (2)

P/bar	x_2	V/(cm^3 mol^{-1})	P/bar	x_2	V/(cm^3 mol^{-1})
		T = 298.15 K			
10.00	0.0270	70.35	45.00	0.1009	68.28
15.00	0.0402	69.96	50.00	0.1115	67.03
20.00	0.0521	69.68	60.00	0.1261	63.80
25.00	0.0624	69.35	70.00	0.1295	63.82
30.00	0.0722	69.09	80.00	0.1298	63.88
35.00	0.0818	68.81	90.00	0.1301	63.77
40.00	0.0914	68.54	100.00	0.1304	63.86
		T = 308.15 K			
10.00	0.0238	71.12	40.00	0.0773	69.93
15.00	0.0347	70.88	45.00	0.0860	69.74
20.00	0.0433	70.67	50.00	0.0946	69.55
25.00	0.0519	70.51	60.00	0.1113	65.02
30.00	0.0604	70.31	70.00	0.1208	64.87
35.00	0.0688	70.12	80.00	0.1210	64.73
		T = 318.15 K			
10.00	0.0215	71.93	45.00	0.0796	70.58
15.00	0.0310	71.72	50.00	0.0878	70.41
20.00	0.0391	71.53	60.00	0.0962	70.42
25.00	0.0472	71.35	70.00	0.0984	70.50
30.00	0.0533	71.18	80.00	0.0986	70.52
35.00	0.0634	70.98	90.00	0.0988	70.54
40.00	0.0714	70.79	100.00	0.0990	70.56

0021-9568/94/1739-0842$04.50/0 © 1994 American Chemical Society

Table 2. Smoothed Values of Liquid-Phase Composition and Liquid Molar Volume V as a Function of Pressure for the Binary System Quinoline (1) + Ethane (2)

P/bar	x_2	V/(cm^3 mol^{-1})	P/bar	x_2	V/(cm^3 mol^{-1})
		T = 298.15			
5.00	0.0350	116.38	30.00	0.2057	105.03
10.00	0.0700	114.07	35.00	0.2395	102.84
15.00	0.1039	111.81	40.00	0.2740	100.59
20.00	0.1381	109.60	45.00	0.3060	98.42
25.00	0.1719	107.28			
		T = 308.15 K			
5.00	0.0365	117.45	35.00	0.2200	105.22
10.00	0.0606	115.78	40.00	0.2401	103.85
15.00	0.0904	113.82	45.00	0.2652	102.24
20.00	0.1230	111.67	50.00	0.2880	100.70
25.00	0.1510	108.09	55.00	0.3120	99.10
30.00	0.1803	107.85			
		T = 318.15 K			
5.00	0.0320	119.02	40.00	0.2079	107.47
10.00	0.0512	117.73	45.00	0.2336	105.83
15.00	0.0787	116.11	50.00	0.2600	104.08
20.00	0.1041	114.37	55.00	0.2801	102.76
25.00	0.1398	112.04	60.00	0.3040	101.40
30.00	0.1559	110.96	65.00	0.3212	100.09
35.00	0.1812	109.30	70.00	0.3423	98.61

Table 3. Smoothed Values of Pressure, Temperature, Composition, and Liquid Molar Volume V of the Liquid$_1$ + Liquid$_2$ + Vapor Locus for the Binary System Dimethyl Sulfoxide (1) + Ethane (2)

		x_2		V/(cm^3 mol^{-1})	
T/K	P/bar	L_1	L_2	V_1	V_2
288.91	35.03[a]	0.0861	0.9924	67.35	78.41
290.15	35.61	0.0875	0.9927	67.78	79.06
291.15	36.48	0.0879	0.9929	68.11	79.92
292.15	37.27	0.0897	0.9930	68.18	80.85
293.15	38.09	0.0906	0.9932	68.26	81.52
294.15	38.90	0.0915	0.9934	68.29	82.73
295.15	39.75	0.0922	0.9936	68.32	83.68
296.15	40.51	0.0933	0.9938	68.44	84.96
297.15	41.24	0.0945	0.9940	68.56	86.45
298.15	42.13	0.0951	0.9943	68.65	87.68
299.15	43.03	0.0960	0.9946	68.74	89.22
300.15	43.90	0.0972	0.9949	68.78	90.97
301.15	44.86	0.0982	0.9953	68.81	92.78
302.15	45.74	0.0992	0.9957	68.86	94.81
303.15	46.62	0.1005	0.9960	68.93	97.28
304.15	47.57	0.1012	0.9962	68.98	100.50
304.51	48.11	0.1018	0.9964	69.02	102.76
305.15	48.45	0.1021	0.9965	69.07	107.05
305.37	48.82[b]	0.1024	0.9967	69.12	114.00

[a] Quadruple point. [b] Type K singular point.

paratus consists of a constant-temperature bath in which is placed a calibrated borosilicate glass equilibrium cell. A mercury displacement pump is used to inject the pure gas component (ethane) from a thermostated steel bomb to the equilibrium cell. The high-pressure (exceeding 70 bar) runs are conducted in a stainless steel high-pressure glass-window cell, containing a vertical bar magnetic stirrer. It is attached to the gas line as before. The rest of the setup and apparatus are the same except that the SS cell is now used in a magnetically stirred acrylic water bath.

For the L_1–V (L_1 = ethane-lean liquid phase, V = vapor phase) isotherms, a known amount of the heavy hydrocarbon was placed in the equilibrium cell and measured amounts of ethane were added to the cell. Using a mass balance, the number of moles of ethane added to the liquid phase was determined. In all cases, the vapor phase was assumed to be pure ethane.

In the case of the L_1–L_2–V (L_2 = ethane-rich liquid phase) runs, the number of moles of ethane in a specific liquid phase was determined from individual runs in which either a small amount or a large quantity of heavy hydrocarbon was initially injected into the cell. By using the results from several runs at different initial loadings of heavy hydrocarbon, the compositions and molar volumes of both the L_1 and L_2 phases could be calculated.

Table 4. Smoothed Values of Pressure, Temperature, Composition, and Liquid Molar Volume V of the Liquid$_1$ + Liquid$_2$ + Vapor Locus for the Binary System Quinoline (1) + Ethane (2)

		x_2		V/(cm^3 mol^{-1})	
T/K	P/bar	L_1	L_2	V_1	V_2
245.09	11.02[a]	0.2184	0.9904	100.51	66.67
248.15	12.50	0.2230	0.9906	101.02	67.04
252.15	14.51	0.2269	0.9909	101.24	68.32
256.15	16.49	0.2318	0.9911	101.30	69.55
260.15	18.38	0.2365	0.9913	101.33	70.78
264.15	20.01	0.2417	0.9916	101.36	72.06
268.15	22.25	0.2458	0.9918	101.39	73.48
272.15	24.18	0.2509	0.9920	101.42	74.97
276.15	26.25	0.2554	0.9922	101.45	76.58
280.15	28.50	0.2602	0.9925	101.47	78.11
284.15	30.08	0.2650	0.9927	101.50	80.04
288.15	33.54	0.2683	0.9929	101.52	82.25
292.15	36.61	0.2725	0.9932	101.55	83.96
296.15	39.97	0.2761	0.9934	101.58	85.50
300.15	43.05	0.2798	0.9936	101.62	88.61
304.15	46.54	0.2834	0.9939	101.66	91.79
308.49	51.15[b]	0.2872	0.9941	101.71	111.45

[a] Quadruple point. [b] Type K singular point.

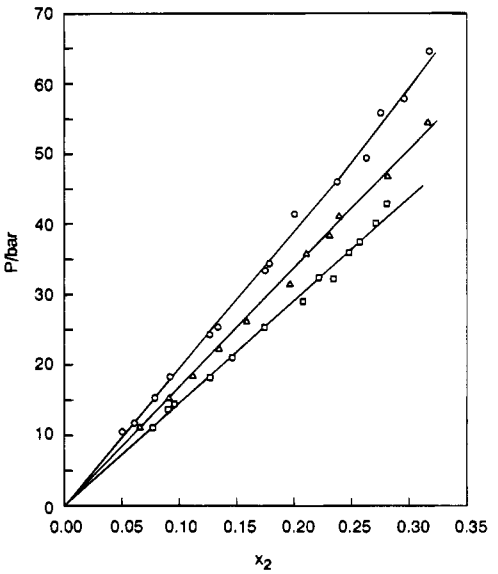

Figure 2. Isothermal pressure versus ethane mole fraction x_2 in ethane (2) + quinoline (1) in the L–V region: □, T = 298.15 K; △, T = 308.15 K; ○, T = 318.15 K.

Temperatures were taken using a platinum resistance thermometer which was accurate to within ±0.03 K. Pressures were measured using Bourdon tube gauges, which were frequently calibrated against an accurate dead weight gauge to an estimated accuracy of ±0.07 bar. The glass equilibrium cell was calibrated and judged to give volumetric readings to an accuracy of ±0.02 cm^3. The high-pressure SS cell had an accuracy of ±0.01 cm^3.

Materials

The gas used in this study is Linde CP grade ethane which has a rated purity of 99.0% minimum. It was purified prior to use in the experimental runs. This gas was passed through consecutive beds of molecular sieves (13A) and an activated charcoal filter and then flashed from the gas cylinder at room temperature into a storage

Table 5. Experimental Results for Dimethyl Sulfoxide (1) + Ethane (2)

			liquid						liquid		
run	P/bar	T/K	x_2	V/(cm^3 mol^{-1})	comment	run	P/bar	T/K	x_2	V/(cm^3 mol^{-1})	comment
1	47.876	304.03	0.9964	100.03	L_1-L_2-V, L_2	9	49.050	305.17	0.9958	113.75	L_1-L_2-V, L_2
	49.123	305.37	0.9968	114.01	K point		47.391	303.46	0.9962	97.87	L_1-L_2-V, L_2
	42.428	298.17	0.9945	87.95	L_1-L_2-V, L_2		42.160	298.21	0.9958	88.59	L_1-L_2-V, L_2
	38.221	293.15	0.9933	81.92	L_1-L_2-V, L_2	10	35.400	289.09	0.9915	78.26	L_1-L_2-V, L_2
	94.920	289.05	0.9925	78.64	L_1-L_2-V, L_2		35.400	289.73	0.9923	78.77	L_1-L_2-V, L_2
2	21.947	318.23	0.0441	71.36	L_1-V		36.305	290.63	0.9929	79.53	L_1-L_2-V, L_2
	31.947	318.23	0.0566	71.21	L_1-V		37.611	292.28	0.9938	81.00	L_1-L_2-V, L_2
	36.847	308.20	0.0657	70.33	L_1-V		38.783	293.70	0.9938	82.36	L_1-L_2-V, L_2
	45.597	308.20	0.0816	69.94	L_1-V		40.430	295.72	0.9942	84.77	L_1-L_2-V, L_2
	35.032	288.91	0.0861	67.35	Q point		41.540	296.90	0.9945	85.89	L_1-L_2-V, L_2
3	10.837	318.18	0.0150	72.12	L_1-V		39.128	294.52	0.9949	83.09	L_1-L_2-V, L_2
	24.491	318.16	0.0369	71.04	L_1-V	11	40.300	295.68	0.9946	85.50	L_1-L_2-V, L_2
	37.007	318.15	0.0656	70.94	L_1-V		41.818	297.57	0.9959	87.85	L_1-L_2-V, L_2
	45.107	318.15	0.0812	70.78	L_1-V		43.335	299.26	0.9957	90.46	L_1-L_2-V, L_2
4	11.613	308.15	0.0181	71.57	L_1-V		44.438	300.54	0.9958	92.88	L_1-L_2-V, L_2
	18.027	308.14	0.0290	71.23	L_1-V		45.678	301.89	0.9964	95.25	L_1-L_2-V, L_2
	24.931	308.15	0.0415	71.16	L_1-V		47.197	303.42	0.9968	99.70	L_1-L_2-V, L_2
	29.900	308.14	0.0595	70.90	L_1-V		48.162	304.22	0.9972	101.70	L_1-L_2-V, L_2
5	8.856	298.15	0.0292	70.29	L_1-V		34.162	289.77	0.9921	77.52	L_1-L_2-V, L_2
	15.407	298.22	0.0408	69.81	L_1-V	12	36.780	289.19	0.9918	77.79	L_1-L_2-V, L_2
	21.820	298.20	0.0571	69.44	L_1-V		37.956	291.59	0.9923	80.31	L_1-L_2-V, L_2
	37.820	298.20	0.0859	68.72	L_1-V		39.610	293.06	0.9928	81.51	L_1-L_2-V, L_2
	42.440	298.21	0.0974	68.29	L_1-L_2-V, L_1		42.093	295.00	0.9926	83.58	L_1-L_2-V, L_2
	42.850	298.86	0.0966	68.29	L_1-L_2-V, L_1		43.956	298.00	0.9934	87.19	L_1-L_2-V, L_2
	42.647	298.64	0.0971	68.25	L_1-L_2-V, L_1		46.645	300.04	0.9939	90.68	L_1-L_2-V, L_2
	42.028	298.11	0.0962	68.20	L_1-L_2-V, L_1		48.780	302.90	0.9945	95.85	L_1-L_2-V, L_2
	42.152	298.08	0.0960	68.25	L_1-L_2-V, L_1		49.024	305.00	0.9950	104.38	L_1-L_2-V, L_2
	41.890	297.64	0.0952	68.21	L_1-L_2-V, L_1		88.960	305.37	0.9967	113.78	K point
	40.028	295.49	0.0953	68.14	L_1-L_2-V, L_1		52.286	318.15	0.0923	70.41	L_1-V
	39.350	292.95	0.0918	68.10	L_1-L_2-V, L_1	13	64.890	318.17	0.0974	70.52	L_1-V
	36.166	290.65	0.0901	67.85	L_1-L_2-V, L_1		74.422	318.16	0.0980	70.57	L_1-V
	35.407	289.82	0.0888	67.89	L_1-L_2-V, L_1		88.420	318.17	0.0980	70.62	L_1-V
	47.476	308.15	0.1275	66.79	L_1-V		96.420	318.17	0.0989	70.60	L_1-V
6	8.097	308.14	0.0202	71.08	L_1-V		104.000	318.17	0.0991	70.64	L_1-V
	13.753	308.14	0.0313	70.86	L_1-V		87.659	308.15	0.2046	61.26	L_1-V
	20.063	308.16	0.0436	70.68	L_1-V		94.694	308.14	0.2094	60.93	L_1-V
	26.718	308.17	0.0542	70.47	L_1-V		104.000	308.16	0.2137	60.64	L_1-V
	32.235	308.16	0.0693	70.05	L_1-V		86.763	298.18	0.2207	59.03	L_1-V
	37.200	308.15	0.0739	69.98	L_1-V		95.591	298.18	0.2242	58.82	L_1-V
	42.580	308.15	0.0821	69.81	L_1-V		104.200	298.17	0.2259	58.74	L_1-V
	46.718	308.15	0.1003	68.83	L_1-V		89.180	290.14	0.2321	57.35	S_1-L-V
	51.063	308.13	0.1091	68.33	L_1-V		57.108	318.16	0.0904	69.97	L_1-V
7	5.020	298.21	0.0141	70.80	L_1-V	14	79.870	318.19	0.1005	70.01	L_1-V
	17.750	298.28	0.0436	69.78	L_1-V		67.453	308.15	0.1550	64.60	L_1-V
	22.030	298.16	0.0557	69.34	L_1-V		76.556	308.15	0.1586	64.62	L_1-V
	27.550	298.18	0.0686	69.09	L_1-V		87.246	308.14	0.1608	64.54	L_1-V
	32.790	298.16	0.0770	69.06	L_1-V		95.521	308.15	0.1636	64.36	L_1-V
	36.994	298.14	0.0855	68.67	L_1-V		103.590	308.16	0.2000	61.61	L_1-V
	42.440	298.17	0.0942	68.49	L_1-L_2-V, L_1		88.620	298.19	0.1727	62.86	L_1-V
	40.370	295.78	0.0922	68.16	L_1-L_2-V, L_1		96.073	298.17	0.1782	62.99	L_1-V
	38.720	293.74	0.0896	68.24	L_1-L_2-V, L_1		104.280	298.19	0.1795	62.93	L_1-V
	36.650	291.19	0.0883	68.30	L_1-L_2-V, L_1		91.591	290.21	0.1849	61.10	S_1-L-V
	35.060	289.19	0.0879	68.32	L_1-L_2-V, L_1		103.660	290.37	0.1853	61.77	S_1-L-V
	48.850	305.34	0.1069	69.03	L_1-L_2-V, L_1		51.314	308.15	0.1025	66.31	L_1-V
8	7.270	318.17	0.0154	71.92	L_1-V	15	61.661	308.15	0.1198	65.08	L_1-V
	12.720	318.13	0.0258	71.85	L_1-V		72.280	308.15	0.1217	64.94	L_1-V
	17.960	318.15	0.0361	71.47	L_1-V		58.280	298.15	0.1292	63.78	L_1-V
	23.480	318.15	0.0445	71.31	L_1-V		68.971	298.15	0.1292	63.81	L_1-V
	28.930	318.17	0.0552	71.16	L_1-V		80.832	298.16	0.1294	63.85	L_1-V
	34.510	318.14	0.0636	70.91	L_1-V		92.280	298.16	0.1309	63.75	L_1-V
	40.720	318.15	0.0730	70.78	L_1-V						
	44.790	318.15	0.0807	70.63	L_1-V						
	48.370	304.84	0.1014	68.61	L_1-L_2-V, L_1						
	46.720	302.88	0.0997	68.49	L_1-L_2-V, L_1						
	44.960	300.89	0.0917	69.11	L_1-L_2-V, L_1						
	42.720	298.51	0.0847	69.09	L_1-L_2-V, L_1						
	40.300	295.78	0.0836	69.05	L_1-L_2-V, L_1						
	34.640	288.91	0.9919	78.65	Q point						

reservoir maintained at about 273 K. The vapor phase was then vented from the reservoir to remove the impurities remaining in the vapor phase after liquefaction from the cylinder, usually about 1/3 of the liquefied ethane. The difference between the bubble and dew point pressures was then measured at 298.15 K and found to be around 14 psia.

Dimethyl sulfoxide and quinoline used are manufactured by Aldrich and have purities of 99.9% and 98%, respectively. These were used as such without further purification. The quinoline density and refractive index were determined in the laboratory at 293.2 K and were found to be 1.093 g/cm^3 and 1.6263, respectively.

Table 6. Experimental Results for Quinoline (1) + Ethane (2)

			liquid						liquid		
run	P/bar	T/K	x_2	V/(cm^3 mol^{-1})	comment	run	P/bar	T/K	x_2	V/(cm^3 mol^{-1})	comment
1	41.541	246.05	0.9901	67.04	L_1–L_2–V, L_2	10	13.465	298.15	0.0907	112.82	L_1–V
	41.678	298.15	0.9935	86.81	L_1–L_2–V, L_2		21.118	298.15	0.1462	109.23	L_1–V
	46.505	304.10	0.9940	91.89	L_1–L_2–V, L_2		34.287	298.15	0.2322	103.84	L_1–V
2	11.070	298.15	0.0766	113.74	L_1–V		40.285	298.15	0.2715	100.67	L_1–V
	18.306	298.15	0.1258	110.79	L_1–V		41.595	298.15	0.2772	101.51	L_1–L_2–V, L_1
	25.545	298.14	0.1730	108.04	L_1–V		33.391	288.15	0.2678	101.14	L_1–L_2–V, L_1
	32.509	298.14	0.2207	104.21	L_1–V		23.945	273.20	0.2543	101.11	L_1–L_2–V, L_1
	41.400	298.13	0.2589	101.82	L_1–L_2–V, L_1		18.705	263.20	0.2411	101.05	L_1–L_2–V, L_1
3	14.170	298.15	0.0949	112.33	L_1–V	11	11.368	249.66	0.2214	100.98	L_1–L_2–V, L_1
	28.990	298.14	0.2071	104.68	L_1–V		12.932	252.84	0.2245	101.20	L_1–L_2–V, L_1
	37.540	298.14	0.2573	101.53	L_1–V		14.309	258.15	0.2292	101.10	L_1–L_2–V, L_1
	41.190	298.14	0.2929	100.99	L_1–L_2–V, L_1		16.371	263.17	0.2333	101.30	L_1–L_2–V, L_1
	42.990	300.13	0.2872	101.16	L_1–L_2–V, L_1		18.790	267.11	0.2334	101.56	L_1–L_2–V, L_1
4	10.308	318.15	0.0490	118.12	L_1–V		21.230	273.05	0.2446	101.70	L_1–L_2–V, L_1
	18.237	318.15	0.0911	115.09	L_1–V		24.020	278.01	0.2625	101.08	L_1–L_2–V, L_1
	25.407	318.15	0.1323	112.23	L_1–V		27.060	283.06	0.2671	101.29	L_1–L_2–V, L_1
	33.474	318.15	0.1746	110.18	L_1–V	12	12.791	249.60	0.9907	68.08	L_1–L_2–V, L_2
	41.334	318.15	0.2012	108.28	L_1–V		12.928	249.62	0.9901	67.35	L_1–L_2–V, L_2
	49.401	318.14	0.2610	104.14	L_1–V		11.483	245.80	0.9902	67.31	L_1–L_2–V, L_2
	58.088	318.15	0.2899	102.06	L_1–V		11.690	245.09	0.9897	66.64	Q point
	66.776	318.14	0.3129	99.74	L_1–V		12.029	249.62	0.9912	66.72	L_1–L_2–V, L_2
	54.641	308.19	0.3180	98.39	L_1–V		13.058	249.69	0.9932	67.61	L_1–L_2–V, L_2
5	11.073	308.15	0.0650	114.18	L_1–V		14.374	253.15	0.9916	68.66	L_1–L_2–V, L_2
	18.380	308.12	0.1118	111.27	L_1–V		16.441	258.16	0.9920	69.96	L_1–L_2–V, L_2
	26.241	308.12	0.1598	108.70	L_1–V		18.788	263.18	0.9922	71.54	L_1–L_2–V, L_2
	31.548	308.12	0.1960	106.31	L_1–V		21.277	267.10	0.9922	73.11	L_1–L_2–V, L_2
	38.583	308.12	0.2314	104.53	L_1–V		24.033	273.05	0.9932	75.07	L_1–L_2–V, L_2
	46.926	308.12	0.2824	100.76	L_1–V		26.921	278.03	0.9929	77.19	L_1–L_2–V, L_2
6	51.162	308.49	0.9918	111.48	K point		28.990	281.15	0.9930	78.54	L_1–L_2–V, L_2
	50.480	307.96	0.9916	111.25	L_1–L_2–V, L_2	13	49.136	306.42	0.9962	96.56	L_1–L_2–V, L_2
	45.020	305.05	0.9911	94.68	L_1–L_2–V, L_2		50.991	308.21	0.9967	110.33	L_1–L_2–V, L_2
	42.175	298.16	0.9907	86.08	L_1–L_2–V, L_2		51.190	308.49	0.9969	111.05	K point
	41.177	292.30	0.9896	83.58	L_1–L_2–V, L_2		51.135	308.35	0.9955	111.03	L_1–L_2–V, L_2
7	11.467	318.13	0.0599	117.91	L_1–V		11.479	245.08	0.9885	66.87	Q point
	24.428	318.13	0.1262	112.97	L_1–V		46.095	303.08	0.9947	90.61	L_1–L_2–V, L_2
	34.357	318.33	0.1794	109.65	L_1–V		46.512	303.45	0.9942	90.23	L_1–L_2–V, L_2
	44.905	318.27	0.2379	105.56	L_1–V		41.967	298.30	0.9925	86.63	L_1–L_2–V, L_2
	41.133	308.16	0.2402	104.23	L_1–V		37.610	293.15	0.9918	84.19	L_1–L_2–V, L_2
	36.149	298.20	0.2480	102.29	L_1–V		33.892	289.52	0.9917	82.87	L_1–L_2–V, L_2
8	15.193	318.18	0.0779	116.50	L_1–V		28.933	281.04	0.9914	78.96	L_1–L_2–V, L_2
	27.603	318.18	0.1421	110.74	L_1–V		25.344	275.06	0.9912	76.24	L_1–L_2–V, L_2
	55.907	318.18	0.2774	103.08	L_1–V		19.619	265.58	0.9910	72.18	L_1–L_2–V, L_2
	62.210	318.18	0.0309	100.74	L_1–V		14.725	253.66	0.9897	69.15	L_1–L_2–V, L_2
	70.520	318.18	0.3328	99.02	L_1–V		13.079	249.15	0.9892	67.88	L_1–L_2–V, L_2
9	13.060	318.15	0.0707	116.63	L_1–V						
	22.373	318.15	0.1161	111.04	L_1–V						
	33.881	318.17	0.1773	107.42	L_1–V						
	42.913	318.17	0.2197	104.92	L_1–V						
	52.773	318.17	0.2706	101.49	L_1–V						
	59.943	318.18	0.2965	99.38	L_1–V						
	50.635	308.18	0.2916	101.82	L_1–L_2–V, L_1						
	48.980	306.28	0.2841	101.64	L_1–L_2–V, L_1						
	46.910	304.18	0.2780	101.69	L_1–L_2–V, L_1						
	41.396	298.16	0.2737	101.50	L_1–L_2–V, L_1						
	59.805	318.17	0.3068	97.93	L_1–V						
	66.907	318.17	0.3247	96.06	L_1–V						

			vapor						vapor		
run	P/bar	T/K	y_2	V/(cm^3 mol^{-1})	Z_g	run	P/bar	T/K	y_2	V/(cm^3 mol^{-1})	Z_g
8	47.740	318.15	0.9992	353.21	0.6581	8	63.177	318.15	0.9943	123.23	0.2943
	54.630	318.15	0.9984	243.22	0.5023		68.982	318.15	0.9928	104.03	0.2713
	59.051	318.15	0.9983	172.40	0.3842						

Results

Tables 1 and 2 present smoothed composition, pressure, temperature, and molar volume data in the vapor–liquid two-phase region at temperatures of 298.15, 308.15, and 318.15 K for ethane + DMSO and ethane + quinoline. Tables 3 and 4 present the liquid–liquid–vapor three-phase data for the two binary systems while Tables 5 and 6 contain the experimental results for the two systems. The standard deviation of the results from the smoothed values of pressure, composition, and liquid molar volume are estimated to be ±0.07 bar, ±0.003 mole fraction, and ±0.32 cm^3 mol^{-1}, respectively, for the ethane + DMSO binary and ±0.07 bar, ±0.005 mole fraction, and ±0.48 cm^3 mol^{-1}, respectively, for the ethane + quinoline binary.

One dew point isotherm was run at 318.15 K, and five dew points were obtained in the pressure range of 48–70 bar. The standard deviation of the dew points from a smoothed dew point composition versus pressure line was less than ±0.001 mole fraction, and the composition of quinoline was generally less than 0.0115. The last five

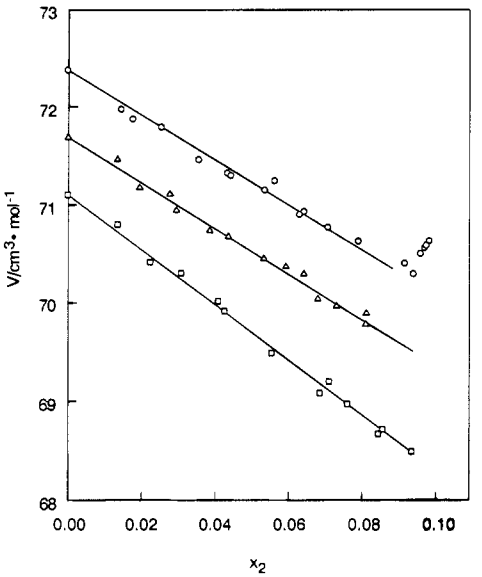

Figure 3. Isothermal liquid molar volume versus ethane mole fraction x_2 in ethane (2) + DMSO (1) in the L–V region: □, T = 298.15 K; △, T = 308.15 K; ○, T = 318.15 K.

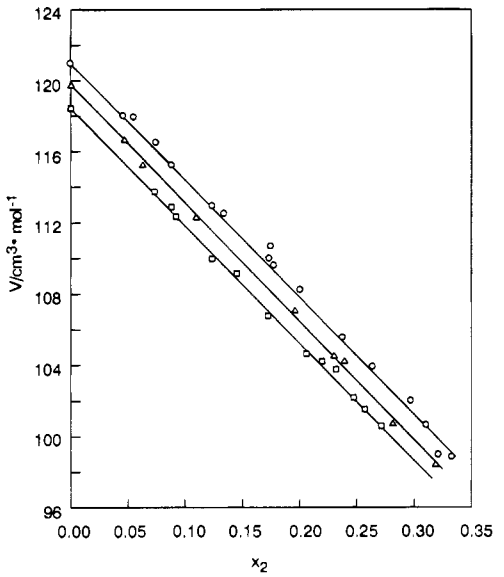

Figure 4. Isothermal liquid molar volume versus ethane mole fraction x_2 in ethane (2) + quinoline (1) in the L–V region: □, T = 298.15 K; △, T = 308.15 K; ○, T = 318.15 K.

points of Table 6 are the actual tabulated values for the dew points.

Figures 1–4 represent the pressure–composition and liquid molar volume–composition diagrams for both systems. Figures 1 and 3 containing the data for the ethane + DMSO system indicate very low solubility of ethane in DMSO relative to ethane solubility as shown in Figures 2 and 4 for the ethane + quinoline system. Such low solubility of ethane in organic solvents appears to be quite rare, but is consistent with the extremely high solubility parameter of DMSO. Figure 1 also shows that the 318.15 K isotherm has a surprisingly high pressure rise over a narrow composition range near 0.098 mole fraction ethane. Figure 3 showing the molar volume of the liquid phase of the ethane + DMSO system also has a sharp increase in liquid molar volume at 318.15 K in the composition range near 0.098 mole fraction ethane. Figure 6 shows no comparable sudden changes in liquid molar volumes for the ethane + quinoline system at any of the three isotherms. Figure 7 shows the liquid molar volumes of both

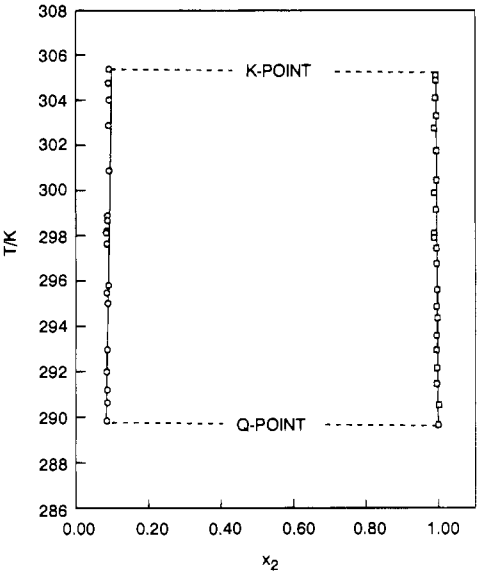

Figure 5. Temperature versus ethane mole fraction x_2 in ethane (2) + DMSO (1) in the L–L–V region: □, L_2 phase; ○, L_1 phase.

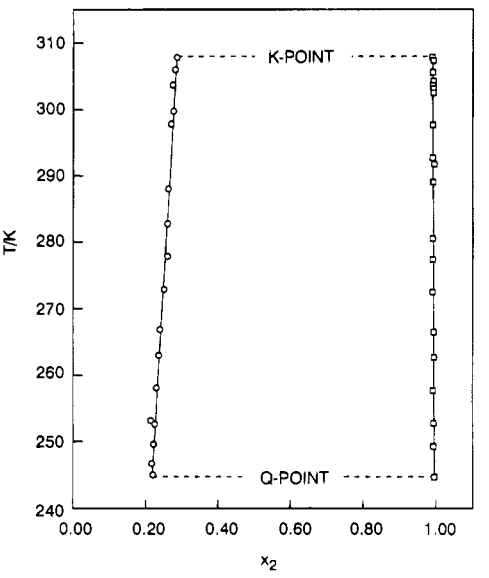

Figure 6. Temperature versus ethane mole fraction x_2 in ethane (2) + quinoline (1) in the L–L–V region: □, L_2 phase; ○, L_1 phase.

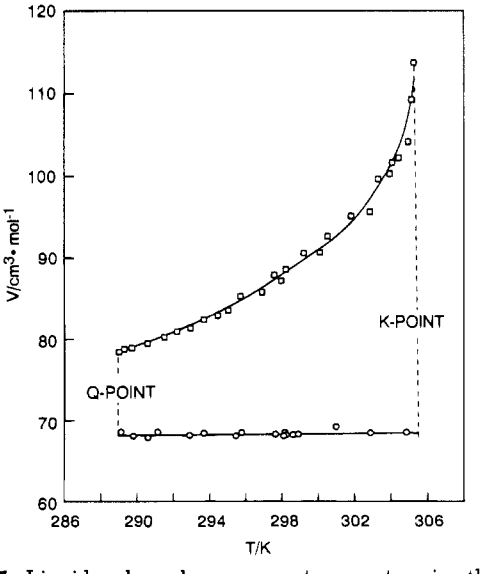

Figure 7. Liquid molar volume versus temperature in ethane (2) + DMSO (1) in the L–L–V region: □, L_2 phase; ○, L_1 phase.

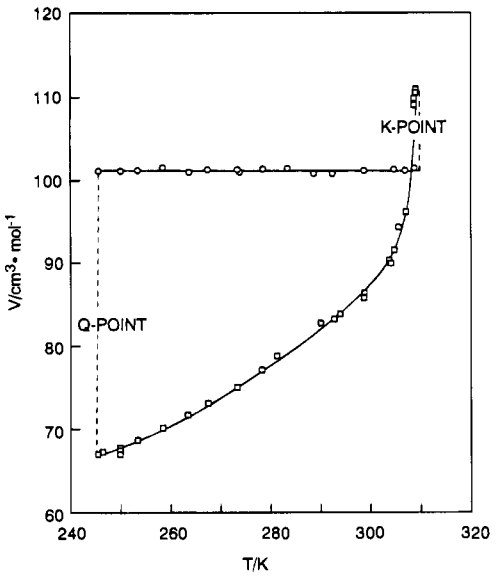

Figure 8. Liquid molar volume versus temperature in ethane (2) + quinoline (1) in the L–L–V region: □, L_2 phase; ○, L_1 phase.

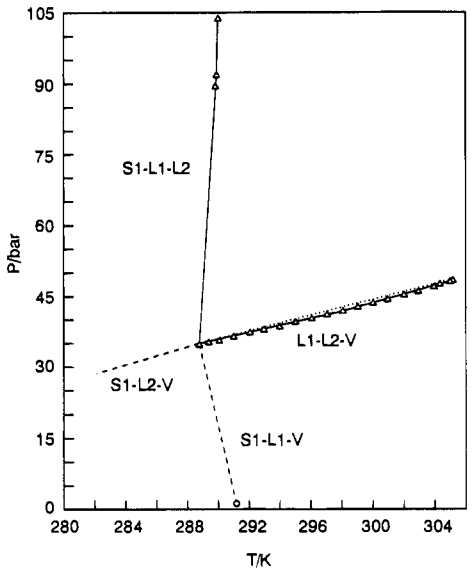

Figure 9. P–T phase diagram of ethane (2) + DMSO (1): ▬, ethane P–T curve; △, experimental data; - - -, expected.

liquid phases in the partial liquid miscibility region for ethane + DMSO while Figure 8 shows comparable data for the ethane + quinoline system.

Figure 9 shows the P–T behavior of the ethane + DMSO system in the quadrupole point region, and Figure 10 shows the P–T behavior in the quadruple point region for the ethane + quinoline system. In the case of the ethane + DMSO system experimental point pressures greater than the quadruple point pressure were obtained along the S_1–L_1–L_2 three-phase line. These points indicate a very high positive shape for the S_1–L_1–L_2 three-phase line. No experimental points were taken along the S_1–L_2–V and S_1–L_1–V lines for the ethane + DMSO system, so these lines are estimated by dashed lines. Figure 10 shows the experimental points obtained along the S_1–L_2–V three-phase line for the ethane + quinoline system and shows the S_1–L_1–L_2 and S_1–L_1–V lines dashed because no experimental data were obtained along these lines.

All the vapor–liquid experimental results were fitted with two models: the Flory–Huggins solution model and the Scatchard modification of regular solution theory. Details of the model calculations can be found in Rodrigues

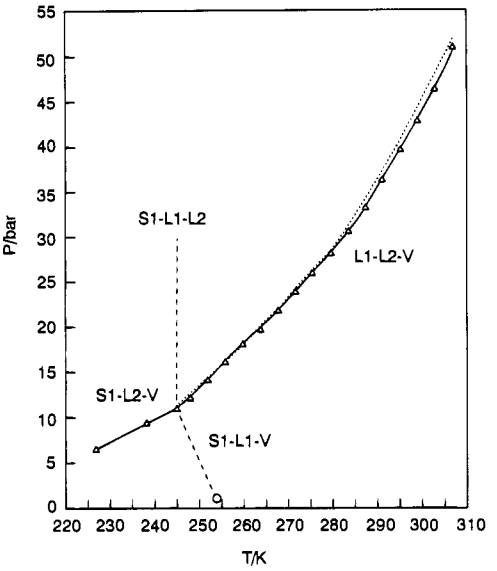

Figure 10. P–T phase diagram of ethane (2) + quinoline (1): ▬, ethane P–T curve; △ experimental data; - - -, expected.

et al. (*10*) and in specific detail in Trehan (*15*). The data from the National Bureau of Standards (*14*) were used for the pure ethane fugacities. The Flory–Huggins model fits the ethane + DMSO results at 298.15 K with a value of the interchange parameter of 3.55 kJ mol^{-1}, and the standard deviation which corresponds to this value of the interchange parameter is ±0.395 bar for the computed fugacities. Corresponding values by the Scatchard model are 2.95 kJ mol^{-1} for the interchange parameter and ±0.444 bar for the standard deviation. For the ethane + quinoline binary the values of the interchange parameter at 298.15 K are 3.42 and 2.58 kJ mol^{-1} for the Flory–Huggins and Scatchard models, respectively. The standard deviations in the computed fugacities are ±0.094 and ±0.172 bar. Although both the solution models fit the data fairly well, the Flory–Huggins model is superior to the Scatchard model.

Literature Cited

(1) Berlin, M. A.; Pluznikova, M. F.; Stepanov, I. N.; Potapov, V. F. *Zh. Prikl. Khim. (Leningrad)* **1980**, *53* (7), 1661.
(2) Brunner, E. *J. Chem. Thermodyn.* **1985**, 871.
(3) Jangkamolkulchai, A.; Arbuckle, M. M.; Luks, K. D. *Fluid Phase Equilib.* **1988**, *40*, 235.
(4) Kohn, J. P.; Kim, Y. J.; Pan, Y. C. *J. Chem. Eng. Data* **1966**, *11*, 333.
(5) Kuenen, J. P.; Robson, W. G. *Philos. Mag.* **1899**, *48*, 180.
(6) Lam, D. H., Jankamolkulchai, A., Luks, K. D. *Fluid Phase Equilib.* **1990**, *59*, 263.
(7) Li, C. G. Ph.D. Thesis, University of Notre Dame, 1990.
(8) Nitschke, T. M.S. Thesis, University of Notre Dame, 1984.
(9) Puri, S.; Kohn, J. P. *J. Chem. Eng. Data* **1970**, *15*, 372.
(10) Rodrigues, A. B.; Kohn, J. P. *J. Chem. Eng. Data* **1967**, *12*, 191.
(11) Rodrigues, A. B.; McCaffrey, D. S.; Kohn, J. P. *J. Chem. Eng. Data* **1968**, *13*, 164.
(12) Shipman, L. M.; Kohn, J. P. *J. Chem. Eng. Data* **1966**, *11*, 176.
(13) Specovius, J.; Leiva, M. A.; Scott, R. L.; Knobler, C. M. *J. Phys. Chem.* **1981**, 2313.
(14) Technical Note 684; U.S. Department of Commerce/NBS: Washington, DC, 1976.
(15) Trehan, A. M.S. Thesis, University of Notre Dame, 1993.
(16) Yamamoto, S.; Ohgaki, K.; Katayama, T. *J. Supercrit. Fluids* **1989**, *2*, 63.
(17) Yamamoto, S.; Ohgaki, K.; Katayama, T. *J. Chem. Eng. Data* **1990**, *35*, 310.

Received for review March 21, 1994. Accepted June 26, 1994.[⊗]

[⊗] Abstract published in *Advance ACS Abstracts,* September 1, 1994.